



A Review on the Process-Structure-Performance of Lanthanum Strontium Cobalt Ferrite Oxide for Solid Oxide Fuel Cells Cathodes

Muhammed Ali S.A.^{1*}, Andanastuti Muchtar², Jarot Raharjo³, Deni Shidqi Khaerudini⁴

¹Fuel Cell Institute,
Universiti Kebangsaan Malaysia, 43600, UKM Bangi, Selangor, MALAYSIA

²Faculty of Engineering and Built Environment,
Universiti Kebangsaan Malaysia, 43600, UKM Bangi, Selangor, MALAYSIA

³Technology Center for Material, National Research and Innovation Agency (BRIN), Building 224, Puspiptek Area,
South Tangerang, Banten, 15314, INDONESIA

⁴Research Center for Physics, National Research and Innovation Agency (BRIN), Kawasan PUSPIPTEK Serpong,
Tangerang Selatan, 15314, Banten, Indonesia

*Corresponding Author

DOI: <https://doi.org/10.30880/ijie.2022.14.02.017>

Received 7 March 2022; Accepted 20 March 2022; Available online 01 June 2022

Abstract: Perovskite-structured $\text{La}_{1-x}\text{Sr}_x\text{Co}_{1-y}\text{Fe}_y\text{O}_{3-\delta}$ (LSCF) is a promising mixed ionic/electronic-conducting material that exhibits excellent electro-catalytic activity toward oxygen reduction and oxygen evolution reactions. LSCF offers potential applications in many processes, such as electrodes for solid oxide fuel cells (SOFCs), oxygen sensors, and dense membrane for oxygen separation and thus have been studied extensively in various fields. However, its physical and electrochemical properties are substantially influenced by dopant concentration, dopant type and processing conditions (synthesis methods, composite cathode effect, fabrication conditions, and chromium poisoning). Understanding and correlating the effect of LSCF composition, its synthesis methods, fabrication conditions, and its parameters are essential to enhance the performance of LSCF cathode for high- to-intermediate temperature SOFC applications. This review emphasizes the importance of enhancing the performance of LSCF cathode by optimizing the influential factors to facilitate and expedite research and development efforts for SOFC commercialization in the near future. Various synthesis and fabrication methods used to prepare and fabricate LSCF and LSCF-based composite cathodes are discussed in detail. Moreover, their pros and cons in optimizing the microstructure of LSCF cathodes are highlighted. Finally, the strategies to improve the long-term microstructural stability and electrochemical performances of the LSCF cathode are discussed.

Keywords: Solid oxide fuel cell, LSCF, microstructure, synthesis, fabrication, degradation

1. Introduction

A solid oxide fuel cell (SOFC) uses hydrogen and oxygen to generate energy [1]. SOFC shows promising performance due to its high fuel-to-energy conversion ratio and fuel flexibility [2]. The current SOFC technology uses ceramic oxide materials and runs between 600°C and 1000°C [3–5]. The use of low temperature from 400 °C to 800 °C has continued to receive considerable interest due their advantages of reduced cost, increased life time, and accelerated warm-up and shutdown time [6]. Reducing the operating temperature can increase the internal resistance of individual

components, specifically the cathode [7, 8]. This is owing to the large activation energy at the cathode side of the SOFC [9]. This phenomenon is called cathodic activation polarization or cathodic activation overpotential.

A cathodic activation loss is a barrier that prevents spontaneous reactions at the cathode interface and electrolyte. Overcoming this barrier necessitates a low activation energy, so ORR can occur fast [10]. The major requirements to minimize these polarization losses are as follow: (1) identifying new promising cathode materials, (2) increasing the surface area of the cathode to enlarge the triple phase boundary (TPB) connectivity, (3) increasing the reactant flow rate or pressure, and (4) adopting a tortuosity or porous microstructure for the cathode to facilitate gas diffusion. Identifying and understanding the influencing factors on these polarization losses is important to improve overall SOFC cathode performance. These include material composition, powder morphology, porosity, and thickness of the cathode, fuel environment (low partial pressure of oxygen gas), operating temperature, and current density [10, 11].

1.1 Different Types of Perovskite-Based Cathode Materials for SOFCs

Due to the high working temperature and activation energy of the oxygen reduction reaction (ORR) on the cathode side of a SOFC, only platinum, gold, and silver are suitable cathode materials [12]. Noble materials, on the other hand, are unsuitable for practical applications due to their high cost, poor electrolyte compatibility, and the generation of volatile oxide (POx) during high-temperature oxidation [13]. As a result, perovskite-structured materials have become popular as cathode materials in SOFCs. Lanthanum strontium manganite (LSM) is the most promising cathode for high-temperature SOFC [14]. Nonetheless, because of its high activation energy for ORR, LSM cathode exhibits high polarization resistance at low temperatures and is thus unsuitable for intermediate temperature (IT) SOFCs below 800 °C [15]. As a result, alternative cathode materials for SOFCs operating at lower temperatures have recently attracted research interest (Table 1) [16].

Table 1 - Different cathode materials for solid oxide fuel cells

Types of cathode materials	Cathode	Power density (mW/cm ²)	Operating temperature (°C)	Reference
Nickelate cathode	La ₂ NiO _{4+δ}	530	750	[17]
	La ₂ Ni _{0.6} Cu _{0.4} O _{4+δ}	120	750	[18]
	Nd _{1.95} NiO _{4+δ}	90	750	[19]
Ferro-cobaltite cathode	La _{0.6} Sr _{0.4} Co _{0.2} Fe _{0.8} O _{3-δ}	930	750	[17]
	Ba _{0.5} Sr _{0.5} Co _{0.8} Fe _{0.2} O _{3-δ}	680	800	[20]
Cobaltite cathode	La _{0.7} Sr _{0.3} CoO _{3-δ}	560	550	[21]
	La _{0.1} Sr _{0.9} Co _{0.9} Nb _{0.1} O _{3-δ}	1478	600	[22]
Sm based cobaltite cathode	Sm _{0.5} Sr _{0.5} Co ₃	400	600	[23]
Gd based cobaltite cathode	Gd _{0.8} Sr _{0.2} CoO ₃	356	700	[24]
Sr based cobaltite cathode	SrCo _{0.95} Sb _{0.05} O _{3-δ}	328	750	[25]
	SrCo _{0.8} Nb _{0.1} Ta _{0.1} O _{3-δ}	1200	500	[26]
	SrSc _{0.175} Nb _{0.025} Co _{0.8} O _{3-δ}	910	500	[27]
K ₂ NiF ₄ type structured cathode	La _{1.96} Sr _{0.04} CuO _{4+δ}	329	700	[28]
	La _{1.96} Sr _{0.04} CuO _{4+δ}	626	700	[28]
	La _{1.2} Sr _{0.8} Co _{0.8} Ni _{0.2} O _{4+δ}	350	600	[29]
Ni doped ferrite cathode	La _{0.8} Sr _{0.2} Fe _{0.6} Ni _{0.4} O _{3-δ}	560	500	[30]
	La _{0.8} Sr _{0.2} Fe _{0.6} Ni _{0.4} O _{3-δ}	600	800	[31]
cobalt-based thermoelectric compound cathode	Ca ₃ Co ₂ O ₆	510	800	[20]

To increase the number of reaction sites outside the TPB region, cathode materials for SOFCs should have mixed ionic-electronic conductivity (MIEC). The main impediment to the development of intermediate-to-low temperature SOFC technologies is the high activation polarization loss associated with the slow ORR at the cathode side at low operating temperatures [32]. As a result, cathode materials with high catalytic activity and compatibility with electrolytes and other components, as well as the ability to perform well at low operating temperatures, must be developed.

Lanthanum strontium cobalt ferrite or $\text{La}_{1-x}\text{Sr}_x\text{Co}_{1-y}\text{Fe}_y\text{O}_{3-\delta}$ (LSCF) perovskite has been extensively researched for its outstanding performance [33–35]. LSCF cathodes have remarkably high oxygen diffusivities ($7.32 \times 10^{-6} \text{ cm}^2/\text{s}$) and oxygen surface exchange coefficients ($1.5 \times 10^{-3} \text{ cm/s}$), at $800 \text{ }^\circ\text{C}$ [36]. In particular, $\text{La}_{0.6}\text{Sr}_{0.4}\text{Co}_{0.2}\text{Fe}_{0.8}\text{O}_{3-\delta}$ (LSCF6428) has a very good electronic conductivity (330 S/cm) and a very low ionic conductivity (0.008 S/cm) at $600 \text{ }^\circ\text{C}$ [37]. As a result, LSCF can be used in a wide range of applications [38]. Thus, LSCF has considerable potential as cathode for IT-SOFC applications. However, its phase formation, surface area, particle size, and overall performance can be influenced by the synthesis and fabrication conditions. Understanding the effects of LSCF composition, characteristics, synthesis processes, and manufacturing conditions is critical to improving SOFC cathode performance.

LSCF-based cathode and its derived composite cathode materials has been extensively studied. Many review articles on LSCF cathode discussed its development, synthesis, fabrication, and factors affecting its degradation [37, 39, 48, 40–47]. Jiang [47] summarized the properties of LSCF for metal-supported SOFCs. Despite their unique position in the development of SOFC technologies, no comprehensive review has been performed on the factors affecting the microstructure of LSCF-based cathode materials. Therefore, the present review intends to fill this knowledge gap and provides data on how to enhance the performance of LSCF-based cathode material by optimizing its microstructure for the development of low-polarization resistance LSCF cathode materials for IT-SOFCs. Critical factors such as composition, synthesis, fabrication, composite cathode, surface segregation, and microstructure degradation and their influence on the microstructural properties and performance of LSCF cathode materials are highlighted. The parameters of different synthesis and fabrication techniques are also discussed. Drawbacks and advancements of composite cathodes are addressed to improve their performance. Finally, the recent advancements to improve the performance of LSCF cathodes are summarized.

2. Factors Affecting the Performance of LSCF Cathodes

The characteristics of the LSCF cathode mainly depend on the nature of A- and B-site dopants, and the microstructure of the final product depends on the synthesis and fabrication techniques (Fig. 1). Microstructure parameters such as micro-macro grain size, low surface area and porosity, and high thickness lead to high polarization resistance. A high surface area nanostructured LSCF cathode has a high electrochemical performance. As a result, these critical factors should be considered in order to improve the performance of the LSCF cathode.

Electrochemical reactions in the SOFC cathode occur between oxygen and electron (e^-) either at the TPB region or at the cathode/gas interface (DPB) [8]. ORR is a collective process caused by several parallel reaction pathways for O^{2-} ion formation [49, 50]. These physio-electrochemical characteristics are governed by different microstructural features. Therefore, optimizing the microstructure of LSCF cathode is necessary to improve its electrochemical performance. Strategies focusing on the microstructure optimization of LSCF cathode materials involve the following: (1) understanding various contributions to the catalytic activity during ORR; (2) quantifying the microstructure in terms of composition, synthesis, and processing conditions (such as operating condition, partial oxygen pressure, and impurities); and (3) identifying the advanced processing conditions and characterization techniques to control the cathode microstructure [51].

2.1 Composition

The LSCF cathode material is a combination of two different perovskite-type-structured $\text{La}_{1-x}\text{Sr}_x\text{CoO}_3$ (LSC) and $\text{La}_{1-x}\text{Sr}_x\text{FeO}_3$ (LSF) cathode materials [52]. Both exhibit MIEC characteristics and have good electrocatalytic activity toward ORR at high temperatures ($800\text{--}1000 \text{ }^\circ\text{C}$). LSCs exhibit higher electrical and ionic conductivity than LSFs [53]. However, LSFs are more chemically stable with electrolyte materials, such as ceria-based and yttria-stabilized zirconia (YSZ), than LSCs [54]. A representation of the LSCF perovskite oxide structure is shown in Fig. 2. The general formula of ABO_3 is associated with perovskite oxide material, where A and B are cations, and O is oxygen anions [40]. In LSCF cathode material, the A-site (x) is doped with Sr^{2+} to enhance the ionic conductivity by forming oxygen vacancies, and the B-site (y) is replaced with a combination of Co^{n+} and Fe^{n+} to improve the electrical conductivity and TEC values [44]. Sr^{2+} is assumed to be located on the La site, whereas Fe^{3+} is on the Co site [55]. Given that Co and Fe are transition metals, the oxidation state can change ($n = 2, 3, 4$), whereas Co^{3+} and Fe^{3+} states are neutral with the lattice [56]. The ionic conductivity of LSCF cathode is closely related to oxygen vacancy concentration with relatively high O^{2-} ion mobility.

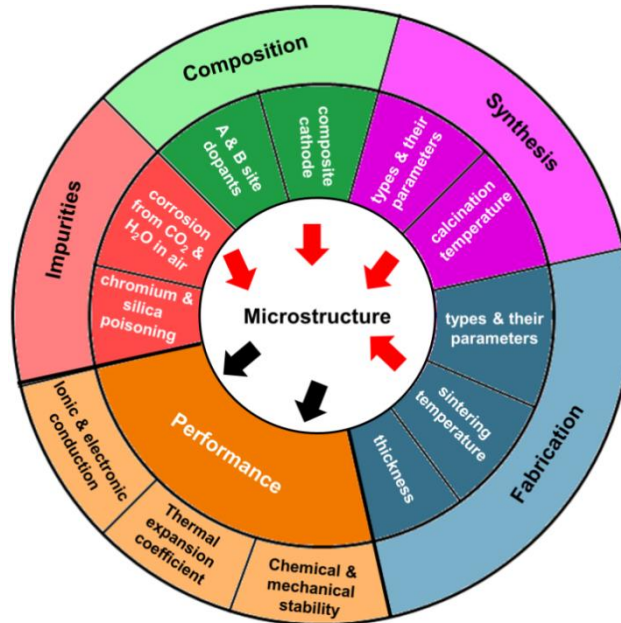


Fig. 1 - Inter-relationship among processing, microstructure, and performance of LSCF cathode

Dutta et al. [57] studied the effect of A-site deficiency ($0 < x \leq 0.5$, $0 < y \leq 0.8$) and B-site doping of different transition metals ($M = \text{Mn}$ or Fe) on the microstructural, thermal, and electrical properties of $\text{La}_{1-x}\text{Sr}_x\text{Co}_{1-y}\text{M}_y\text{O}_3$. The results revealed that $\text{La}_{0.5}\text{Sr}_{0.5}\text{Co}_{0.8}\text{Fe}_{0.2}\text{O}_3$ showed good sinterability with distinct grain boundaries when sintered between $1000\text{ }^\circ\text{C}$ and $1100\text{ }^\circ\text{C}$. Heavy A-site doping (Sr) and the presence of cobalt and iron are beneficial to the sintering process due to liquid-phase sintering and nanocrystal precipitation at the time of recrystallization (Table 2). Moreover, the structure, ionic, electrical conductivity, and TEC of LSCF depend on the dopant concentration and temperature. Tai et al. [58] studied the dependence of structure, electrical conductivity, and TEC of A-site deficient $\text{La}_{1-x}\text{Sr}_x\text{Co}_{0.2}\text{Fe}_{0.8}\text{O}_{3-\delta}$ ($0 \leq x \leq 0.8$) and Co-rich $\text{La}_{0.8}\text{Sr}_{0.2}\text{Co}_{1-y}\text{Fe}_y\text{O}_{3-\delta}$ ($0 \leq y \leq 1$)[59]. Three different perovskite structures were observed for the LSCF cathode with varying Sr dopant levels at room temperature. $\text{La}_{1-x}\text{Sr}_x\text{Co}_{0.2}\text{Fe}_{0.8}\text{O}_{3-\delta}$ cathode displays three structures, that is, orthorhombic ($0 \leq x \leq 0.2$), rhombohedral ($0.3 \leq x \leq 0.8$), and cubic structures ($x > 0.8$).

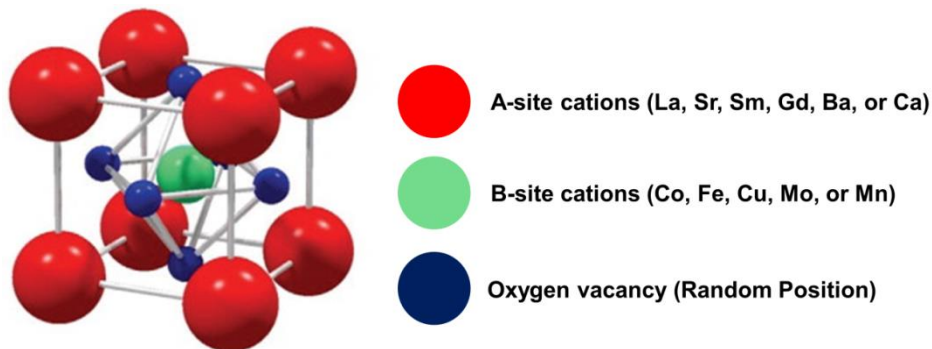
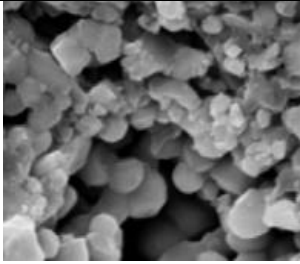
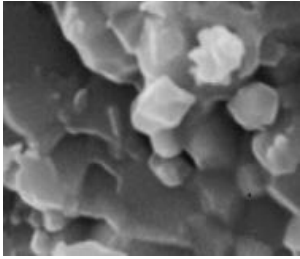
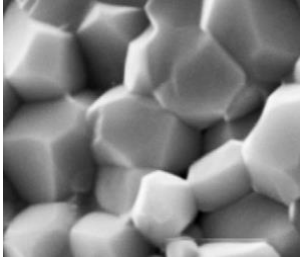
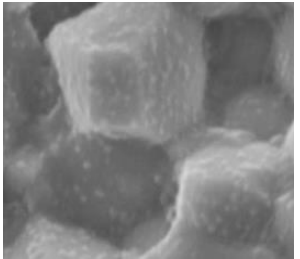


Fig. 2 - Schematic of the perovskite oxide (ABO_3) structure [60]

When the transition metal Co is used, it is more chemically compatible with ceria-doped electrolyte, whereas Fe produces a similar TEC value and improves electronic conductivity [61, 62]. In Sr-doped LaFeO_3 cathode with Co-rich perovskite structure, the electrical conductivity of $\text{La}_{0.8}\text{Sr}_{0.2}\text{Co}_{0.9}\text{Fe}_{0.1}\text{O}_{3-\delta}$ increases to as high as $\sim 1200\text{ S/cm}$ at $550\text{ }^\circ\text{C}$. However, the TEC of Co-rich perovskites is not chemically stable with ceria-doped electrolytes. The average TEC value of $\text{La}_{0.8}\text{Sr}_{0.2}\text{Co}_{0.9}\text{Fe}_{0.1}\text{O}_{3-\delta}$ is $20.1 \times 10^{-6}\text{ K}^{-1}$, which is higher than those of YSZ, samarium-doped ceria (SDC), and gadolinium-doped ceria (GDC) (Table 3). When the Fe content is increased to $y = 0.8$, the TEC value decreases to $15.3 \times 10^{-6}\text{ K}^{-1}$. The TEC value of SDC is $12.9 \times 10^{-6}\text{ K}^{-1}$ [63]. Therefore, Fe-rich perovskite is more chemically compatible with ceria-doped electrolytes than Co-rich perovskite. Moreover, the presence of Co and Fe cations helps in the sintering of the LSCF cathode system.

Table 2 - Dependence of microstructure and electrical properties at 800 °C on the A-and B-site compositions

Composition	Sintering temperature (°C)	Electrical conductivity (S/cm)	Area specific resistance (ASR, Ωcm ²)	Surface morphology (SEM images, 500 nm)
La _{0.65} Sr _{0.3} MnO ₃	1100	19	2.85	
La _{0.8} Sr _{0.2} FeO ₃	1100	4	7.61	
La _{0.8} Sr _{0.2} Co _{0.8} Fe _{0.2} O ₃	1100	24	0.339	
La _{0.5} Sr _{0.5} Co _{0.8} Fe _{0.2} O ₃	1100	115	0.211	

2.2 Synthesis Methods

The chosen synthesis method should yield the desired composition and fine microstructure to achieve the enhanced performance of the LSCF cathode. For example, the performance of the final cathode depends on the powder properties of the initially synthesized cathode powders. Moreover, the cathode performance is substantially influenced by the calcination temperatures of the starting powder and the microstructure of the resulting LSCF cathode in the sintered layer [64]. Table 4 shows that the calcination temperature, surface area, and area-specific resistance (ASR) of the LSCF cathode are dependent on the synthesis method. Microstructures produced by varying preparation procedures and calcination temperatures directly affect the specific surface area and ASR of LSCF cathodes with the same stoichiometry. The solid-state reaction was the first method utilized to generate ceramic powders due to its excellent selectivity, high yield, lack of solvents, and simplicity [65]. However, this process requires repeated cycles of milling, calcination at elevated temperatures (> 1000 °C), and grinding to produce powders with a high electrical conductivity. This procedure introduces impurities into the SOFC cathode, resulting in decreased catalytic activity and higher ASR. Wet-chemical synthesis techniques, such as spray pyrolysis [66], sol-gel process [67], glycine–nitrate process (GNP) [68], ethylenediaminetetraacetic acid–citrate process [69], and co-precipitation process [70], were adopted for the preparation of LSCF cathode powders to overcome these disadvantages. The powders from these methods usually show relatively good performance due to the atomic-scale homogeneous mixing of raw materials.

Table 3 - Electrical conductivity and thermal expansion coefficient (TEC) of LSCF cathode materials with different compositions

Composition	Electrical conductivity (S/cm at °C)	TEC		Reference
		TEC value ($\times 10^{-6} \text{ K}^{-1}$)	Temperature range (°C)	
$\text{La}_{0.6}\text{Sr}_{0.4}\text{CoO}_{3-\delta}$	2204 at 600	20	25–850	[53, 71]
$\text{La}_{0.6}\text{Sr}_{0.4}\text{FeO}_{3-\delta}$	128 at 800	16.3	30–1000	[54]
$\text{La}_{0.9}\text{Sr}_{0.1}\text{Co}_{0.2}\text{Fe}_{0.8}\text{O}_{3-\delta}$	70 at 1000	16	300–900	[58]
$\text{La}_{0.8}\text{Sr}_{0.2}\text{Co}_{0.2}\text{Fe}_{0.8}\text{O}_{3-\delta}$	190 at 800	15.4	100–800	[58, 72]
$\text{La}_{0.7}\text{Sr}_{0.3}\text{Co}_{0.2}\text{Fe}_{0.8}\text{O}_{3-\delta}$	240 at 600	14.6	100–700	[58]
$\text{La}_{0.6}\text{Sr}_{0.4}\text{Co}_{0.2}\text{Fe}_{0.8}\text{O}_{3-\delta}$	330 at 550	15.3	100–600	[58]
$\text{La}_{0.6}\text{Sr}_{0.4}\text{Co}_{0.2}\text{Fe}_{0.8}\text{O}_{3-\delta}$	301 at 800	17.5	100–400	[54]
$\text{La}_{0.4}\text{Sr}_{0.6}\text{Co}_{0.2}\text{Fe}_{0.8}\text{O}_{3-\delta}$	316 at 500	13.7	100–500	[73]
$\text{La}_{0.2}\text{Sr}_{0.8}\text{Co}_{0.2}\text{Fe}_{0.8}\text{O}_{3-\delta}$	-	15.9	100–500	[73]
$\text{La}_{0.6}\text{Sr}_{0.4}\text{Co}_{0.5}\text{Fe}_{0.5}\text{O}_{3-\delta}$	489	20.3	30–1000	[54]
$\text{La}_{0.6}\text{Sr}_{0.4}\text{Co}_{0.8}\text{Fe}_{0.2}\text{O}_{3-\delta}$	296	21.4	30–1000	[62, 74]
$\text{La}_{0.8}\text{Sr}_{0.2}\text{Co}_{0.1}\text{Fe}_{0.9}\text{O}_{3-\delta}$	100 at 1000	14.5	200–900	[59]
$\text{La}_{0.8}\text{Sr}_{0.2}\text{Co}_{0.2}\text{Fe}_{0.8}\text{O}_{3-\delta}$	120 at 1000	15.4	100–800	[59]
$\text{La}_{0.8}\text{Sr}_{0.2}\text{Co}_{0.3}\text{Fe}_{0.7}\text{O}_{3-\delta}$	200 at 1000	16.5	100–900	[59]
$\text{La}_{0.8}\text{Sr}_{0.2}\text{Co}_{0.4}\text{Fe}_{0.6}\text{O}_{3-\delta}$	250 at 1000	17.6	100–900	[59]
$\text{La}_{0.8}\text{Sr}_{0.2}\text{Co}_{0.5}\text{Fe}_{0.5}\text{O}_{3-\delta}$	260 at 900	18.7	100–900	[59]
$\text{La}_{0.8}\text{Sr}_{0.2}\text{Co}_{0.6}\text{Fe}_{0.4}\text{O}_{3-\delta}$	450 at 900	20	100–900	[59]
$\text{La}_{0.8}\text{Sr}_{0.2}\text{Co}_{0.7}\text{Fe}_{0.3}\text{O}_{3-\delta}$	760 at 800	20.3	100–900	[59]
$\text{La}_{0.8}\text{Sr}_{0.2}\text{Co}_{0.8}\text{Fe}_{0.2}\text{O}_{3-\delta}$	1100 at 600	20.7	100–900	[59]
$\text{La}_{0.8}\text{Sr}_{0.2}\text{Co}_{0.9}\text{Fe}_{0.1}\text{O}_{3-\delta}$	1200 at 550	20.1	100–900	[59]
YSZ	-	13	26–1650	[75]
SDC	-	12.9	30–1000	[63]
GDC	-	11.5	30–1050	[76]

Different synthesis routes have been explored and compared to identify a suitable and cost-effective method to produce LSCF cathode powders for SOFC applications. Figure 3 shows the LSCF cathode powders with diverse morphological characteristics prepared through different techniques and calcined at different temperatures. Liu et al. [61] reported the effects of three different synthesis techniques, namely, ethylenediamine tetra-acetate (EDTA)/citrate, citrate, and solid-state reaction, on the physical and electrochemical properties of LSCF6428 powder. Overall, the LSCF powder made with EDTA/citrate showed better phase formation, smaller grain size, and better electrical performance than the solid-state reaction powder. The power density of the citrate-produced LSCF powder is 189 mW/m², nearly 46% higher than the solid-state reaction powder (135 mW/m²). Similarly, Qi et al. [77] also reported the effect of four different synthesis methods: (1) citrate method, (2) solid-state method, (3) spray-pyrolysis, and (4) coprecipitation for $\text{La}_{0.8}\text{Sr}_{0.2}\text{Co}_{0.6}\text{Fe}_{0.4}\text{O}_{3-\delta}$ (LSCF8264) cathode and found that these techniques considerably influenced the morphological and oxygen ion transport properties of the cathode. Except for coprecipitation, which caused a substantial strontium shortage in the prepared LSCF8264 due to repeated filtration and washing procedures. In summary, the citrate gel technique may be used to produce LSCF powders with optimum physical properties and pure structure.

Table 4 - Dependence of calcination temperature, surface area, and area-specific resistance (ARS) of LSCF6428 cathode on the preparation method

Method	Calcination Temperature (°C)	Surface area (m ² /g)	ASR (Ω cm ² at °C)	Reference
Commercial (fuel cell materials)		4–8	0.7 at 850	[78]
Solid state reaction	1100	0.8	1.47 at 950	[61, 70]
Coprecipitation	1000		0.76 at 850	[78]
Sol-gel (citrate complexing process)	900	14.3	1.115 at 950	[61, 79]
CECP	700	14.6		[80]
Modified sol-gel process	900	7		[67]
GNP	900		0.67 at 650	[81]
Modified GNP	900		0.36 at 650	[81]
Gel casting technique	950	8.07		[79]
Spray pyrolysis	1000		1.36 at 700	[66]
Citrate–hydrothermal synthesis	900	5.2	0.34 at 750	[82]
Microwave-assisted sol-gel method	900		0.2 at 700	[83]

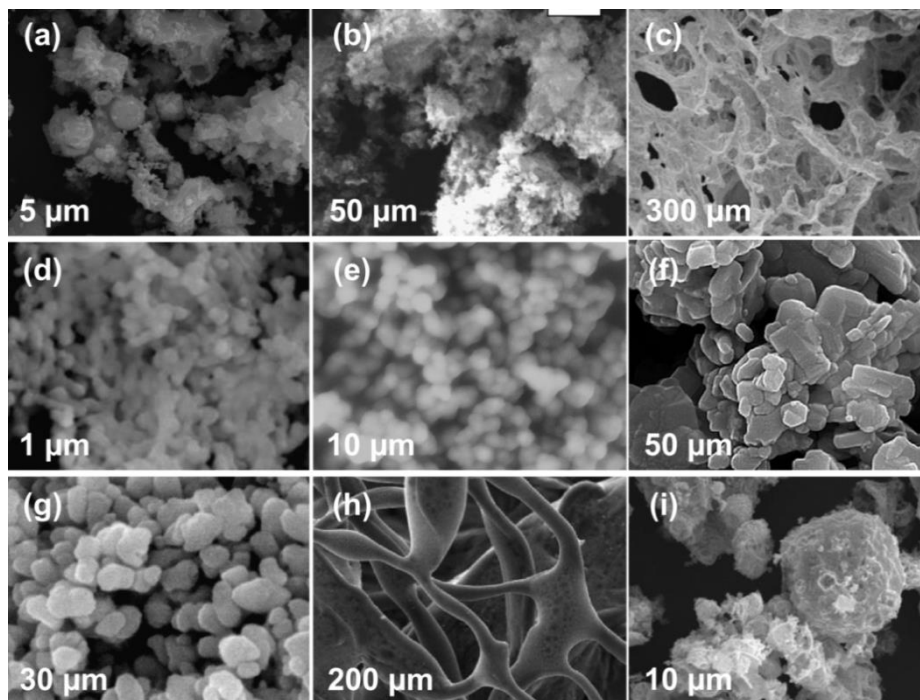


Fig. 3 - SEM images of LSCF6428 cathode powders synthesized by different methods, that is, (a) citrate–hydrothermal synthesis [82], (b) sol-gel with EDTA and citric acid [84], (c) auto combustion with NH₄NO₃ [85], (d) modified sol-gel [67], (e) microwave-assisted sol-gel [83], (f) coprecipitation [78], (g) polymeric complexing combustion [80], (h) modified GNP [81], and (i) GNP [64]

The sensitivity of the processing technique shown in the examples above influences the performance of the LSCF cathode. All methods have an effect on ultimate electrical conductivity based on powder properties and impurity levels. Because of the differences in powder morphology, each process produces a unique set of sintering conditions and

microstructures [77]. Understanding and controlling the parameters involved in each synthesis method are important for the composition and morphology of the resulting powder. The details of the important parameters for different synthesis methods are listed in Table 5. Given that the sensitivity of preparation method and its parameters can seriously influence the performance of LSCF cathodes, the selection of a suitable synthesis type and its effects should be considered to achieve maximum efficiency.

Table 5 - Important parameters of different synthesis processes

Method	Parameters
Solid state reaction	Ball to powder mass ratio; Milling time; Milling speed; Solvent type
Sol-gel	Complexant type and its content (hydrochloric acid, acetic acid or acetyl acetone); Solvent content; Catalyst to control both the hydrolysis and condensation rates
Polymeric complexing combustion	Type and content of chelating agents (citric acid, ascorbic acid, polyvinyl alcohol, formic acid or polyethylene glycol); Adjustment of Ph value; Solvent types (water, ethylene glycol or 2-methoxyethanol)
Spray pyrolysis	Spray rate of carrier gas; Deposition time and needle to substrate distance; Size of droplets; Solvent composition and concentration; Ratio of the air-gas mixture; Flame temperature; Frequency of the atomizer; Applied voltage
Coprecipitation process	Precipitant concentration; Adjustment of Ph value; Reaction temperature
Combustion process	Fuel type and its content (glycine, urea, alanine or carbonylhydrazide); Adjustment of Ph value; Dispersant content; Combustion aid
Hydrothermal process	Mineralizer (alkaline hydroxides or alkaline carbonate); Reaction temperature; Solvent type (ethanol or methanol)
Microwave irradiation	Rate of microwave heating; Electric field distribution; Intensity of the electric field; Location of sample in the microwave oven

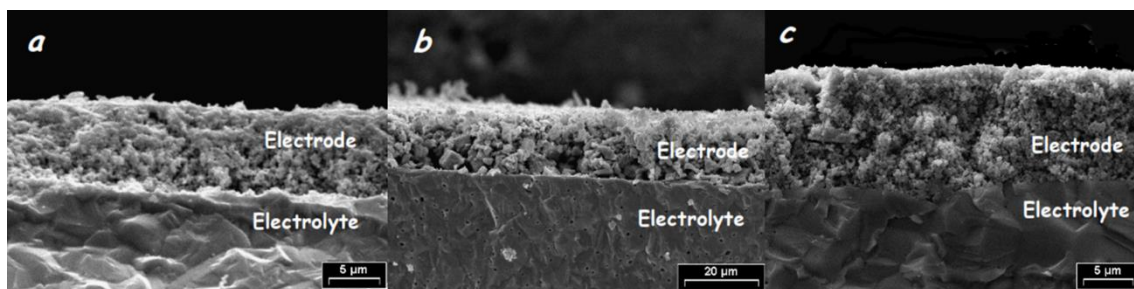
2.3 Fabrication Methods

High performance, long-term durability, and chemical stability in an oxidizing environment can be achieved for the LSCF cathode by choosing the appropriate fabrication techniques and conditions. Several methods, such as uniaxial pressing, painting, printing technique, dip coating, extrusion/co-extrusion, wet powder spraying, spray pyrolysis, vacuum deposition, and impregnation/infiltration, typically followed by drying, decomposition, and high-temperature sintering have been employed to produce LSCF cathode layers onto the substrate [86–91]. Each method has its own set of parameters that must be optimized to attain the desired performance (Table 6). A number of these methods are readily adaptable to LSCF cathode layer fabrication. The most widely used methods for LSCF cathodes are uniaxial pressing, tape casting, painting, dip coating, and screen printing due to their low cost and simplicity [92]. The ideal process of fabricating a cathode layer starts from the synthesized powder and its powder characteristics. The physical and surface properties of the synthesized powder strongly depend on the selected synthesis technique, which in turn influences the subsequent fabrication of the cathode layer. The particle size, shape, distribution, degree of agglomeration, chemical composition, and purity of the starting powder are the main factors that affect the quality of the prepared cathode slurry, suspension, or ink [93]. Some of the ink or slurry formulations for fabricating LSCF cathode layers have been optimized, such as dip coating and brush painting [90], tap casting [87], and screen printable inks [94].

A major consideration in cathode layer fabrication is the effect on the microstructure of the resulting layers. Microstructure aspects related to grain size and porosity greatly influence the transport properties and ORR rate. Coarse microstructures promote ionic and electronic conductivities while fine microstructures produce large specific surface areas and hence many reaction sites [87]. Owing to these fabrication–microstructure–performance interrelationships, optimization must be performed on the composition and synthesis methods used to produce the initial cathode powder and the fabrication conditions used to produce the final cathode layers. Many researchers concentrated on increasing LSCF cathode performance by modifying their microstructure for ORR [95–100]. Therefore, selecting the most appropriate fabrication techniques and conditions for cathode layer fabrication has gained considerable importance. Baqué et al. [89] investigated the effects of the fabrication techniques (i.e., spray painting, spin and dip coating) on the electrical properties of $\text{La}_{0.4}\text{Sr}_{0.6}\text{Co}_{0.8}\text{Fe}_{0.2}\text{O}_{3-\delta}$ (LSCF4682) films and obtained films with different porous microstructures and layer thicknesses (Fig. 4). The same study found that the ASR of LSCF4682 cathode films is heavily influenced by their microstructure, which is determined by the synthesis conditions and fabrication procedures.

Table 6 - Key parameters of different fabrication techniques

Technique	Thickness	Parameter
Uniaxial pressing	>0.5 mm	Pressure; Holding time
Tape casting	>10 μm	Slurry composition; Tape casting speed; De-airing time; Gap between the doctor blade; Carrier film
Screen printing	>5 μm	Slurry composition; Squeegee hardness; Squeegee pressure; Printing speed; Mesh size; Snap-off distance
Dip coating	>1 μm	Precursor or slurry composition; Lifting speed and dwelling time; Curing time and temperature between each dip coating step; Dipping number to achieve the desired thickness
Brush painting	>1 μm	Slurry composition; Curing time and temperature between each painting step; Painting number to achieve the desired thickness
Extrusion	100 μm to mm	Density and rheological properties of the ceramic paste (plasticity); Processing temperature; Wall thickness (outer diameter); Screw speed; Piston extrusion pressure; Die design
Electrophoretic deposition	<5 μm	Suspension properties (particle size, conductivity, viscosity, stability, and concentration of solid content); Dielectric constant of the liquid; Zeta potential; Conductivity of substrate; Deposition time; Applied voltage
Plasma spraying	>20 mm	Power (kW); Torch current (A); Plasma primary and secondary gas composition (L/min); Stand-off distance (mm); Feedstock carrier gas (L/min); Powder feed rate (rpm); Surface speed (rpm); Transverse speed (mm/s); Nozzle diameter
Spray pyrolysis	1 μm	Atomization method; Deposition temperature; Salt composition; Solution-flow rate; Air pressure; Ratio of deposition temperature to solvent boiling point
Infiltration	-	Sintered porous preform; Slurry of nano-sized particles


Fig. 4 - SEM images of LSCF4682 cathode films deposited by different fabrication techniques: (a) Dip coating; (b) spray painting; (c) spin coating [89]

Fabrication conditions (sintering temperature, ramping rate, dwell time, thickness, and solid content) ultimately affect the cathode microstructure and its final performance. da Conceição et al. [101] investigated the influence of sintering temperature on the performance of the LSCF cathode and found a clear relationship between the electrical conductivity and densification of the pellets. When sintering was performed at temperatures ranging from 950 °C to 1100 °C for 4 h to obtain bulk LSCF cathode samples, the porosity of the samples decreases with the increasing sintering temperature. The highly dense samples obtained by sintering at 1100 °C exhibited a large decrease in electrical conductivity because of the changes in their conduction mechanism and microstructure. The important influences of lanthanum content, sintering temperature, and dwell time on the performance of LSCF cathodes were reported by Mobius et al. [102]. It was found that the sintering temperature exerts a more serious effect on the microstructure and densification of the cathode than dwell time. However, lanthanum content does not substantially influence the final sintering temperature and dwell time.

Leng et al. [68] reported the influence of sintering temperature on the performance of LSCF6428 cathodes. Good performance can be achieved under fine grain size, sufficient porosity, good bonding between grains, and good adhesion between the cathode and electrolyte. The sample sintered at 975 °C showed lower interfacial polarization resistance of 1.2 Ω cm² at 600 °C compared with the sample sintered at a high temperature. This performance difference was attributed to the microstructure of the sintered LSCF6428 cathode layers. The cathode interfacial polarization resistance also depends on the thickness of the LSCF cathode layer [103]. Han et al. [104] investigated the effect of ink concentration, porosity, and thickness of the LSCF layer on the electrochemical performance of the resulting cathode by preparing a LSCF cathode layer using a commercial low-price inkjet printer (Fig. 5). The findings showed that using a high concentration (i.e., high solid content) of ink resulted in large cracks on the surface of the printed cathode layers and poor performance possibly because of changes in the microstructure of the cathode film with the increasing thickness. Han et al. [104] reported that thick cathode layers exhibit relatively better performance than thin cathode layers. This finding can be attributed to the increased availability of active sites for the electrochemical reaction caused by the increase in cathode layer thickness. This improvement is only valid up to a particular electrode microstructure thickness. If the cathode is thicker than this, it functions as a semi-infinite electrode, and the ASR remains constant. The pore size in the printed layer and the mass diffusion through the cathode layer are also essential factors influencing LSCF cathode and fuel cell performance.

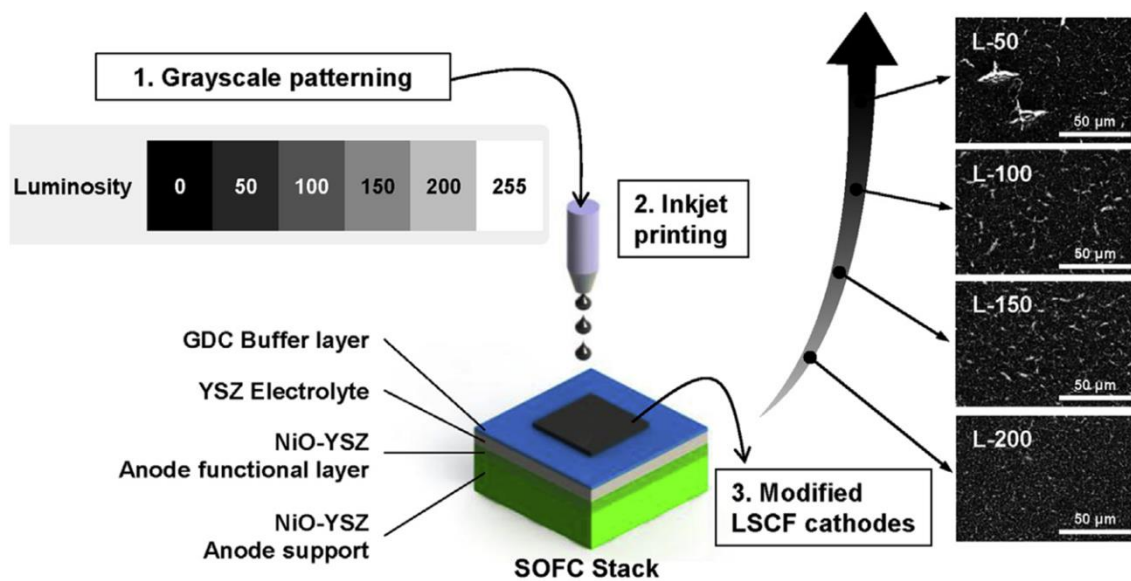


Fig. 5 - Schematic representation of LSCF6428 cathode fabrication using the inkjet printing method [104]

3. LSCF-based Composite Cathode

Although LSCF is an outstanding MIEC material, a second-phase pure-oxygen ion conductor can significantly increase performance and durability [35]. Composite cathode powders are usually prepared by mixing a specific weight percentage of the pure cathode material with a pure ionic conductor electrolyte. LSCF cathodes are chemically and thermally compatible with ceria-based electrolytes such as SDC, and GDC, another popular electrolyte for SOFC [105–108]. The initial idea is to develop a composite cathode to enhance oxygen transport property, increase the TPB, and subsequently improve the electrochemical properties of LSCF cathode material [109]. Shaule et al. [110] reported that the oxygen permeation flux of LSCF-SDC composites is one order of magnitude higher than that of single-phase LSCF cathodes. This variation is possibly due to the high ionic conductivity of the electrolyte materials, which effectively introduces additional oxygen ion vacancies to the LSCF cathode structure and improves the oxygen diffusion rate of the composite. However, the electrochemical properties of LSCF-based composite cathodes can be remarkably influenced by their composition and the synthesis techniques used to prepare the starting powder and composite cathode. Table 7 lists the effects of composition and synthesis technique on the electrochemical properties of LSCF-based composite cathodes.

Cesario et al. [111] studied the effect of LSCF cathode synthesis method on the performance of the final LSCF-SDC composite cathode. Various powder morphologies with different levels of agglomeration and particle size distribution were observed. They concluded that LSCF powders synthesized from the modified Pechini method exhibited an ASR four times lower than that of LSCF powders obtained through microwave combustion. In another study, the presence of slight impurities in the LSCF starting powder seriously affects its electrical performance [112]. Therefore, the electrochemical properties of LSCF-SDC composite cathodes are closely related to the purity of the starting LSCF cathode powders. The fabrication technique used to prepare the LSCF-based composite cathode also influences its final performance. Shen et al. [107] used three different techniques, i.e., mixing, infiltration, and dip coating, to prepare LSCF-SDC composite cathode layers and found that each method results in different

microstructures and TPB lengths. Compared with the two other techniques, dip coating yielded the best morphology and highest electrical performance.

Table 7 - LSCF-based composite cathode materials

Composite cathode	Synthesis technique		ASR, Ωcm^2 at ($^{\circ}\text{C}$)	Reference
	LSCF powder	Composite cathode		
$\text{La}_{0.8}\text{Sr}_{0.2}\text{Co}_{0.5}\text{Fe}_{0.5}\text{O}_3 + \text{Ce}_{0.8}\text{Gd}_{0.2}\text{O}_2$	Modified polymer-assisted combustion	infiltration	0.06 at 750	[113]
$\text{La}_{0.8}\text{Sr}_{0.2}\text{Co}_{0.2}\text{Fe}_{0.8}\text{O}_{3-\delta} + \text{Ce}_{0.8}\text{Gd}_{0.2}\text{O}_2$	LSCF precursor solution-fiber	Infiltration	0.29 at 750	[114]
75 wt. % $\text{La}_{0.6}\text{Sr}_{0.4}\text{Co}_{0.2}\text{Fe}_{0.8}\text{O}_{3-\delta} + \text{Ce}_{0.9}\text{Gd}_{0.1}\text{O}_{1.95}$	Freeze-drying precursor method	Mixing	0.27 at 600	[115]
50 wt. % $\text{La}_{0.6}\text{Sr}_{0.4}\text{Co}_{0.2}\text{Fe}_{0.8}\text{O}_{3-\delta} + \text{Ce}_{0.9}\text{Gd}_{0.1}\text{O}_{1.95}$	Spray-pyrolysis	spray-pyrolysis	0.032 at 600	[116]
50 wt. % $\text{La}_{0.6}\text{Sr}_{0.4}\text{Co}_{0.2}\text{Fe}_{0.8}\text{O}_{3-\delta} + \text{Ce}_{0.9}\text{Gd}_{0.1}\text{O}_2 + 1 \text{ wt. \% CuO}$	Commercial (fuel cell materials)	Mixing + infiltration of CuO	0.32 at 650	[117]
50 wt. % $\text{La}_{0.58}\text{Sr}_{0.4}\text{Co}_{0.2}\text{Fe}_{0.8}\text{O}_3 + \text{Ce}_{0.8}\text{Gd}_{0.2}\text{O}_{2-x} \& 2 \text{ wt. \% V}_2\text{O}_5$	Glycine-nitrate process	Mixing		[118]
50 wt. % $\text{La}_{0.58}\text{Sr}_{0.4}\text{Co}_{0.2}\text{Fe}_{0.8}\text{O}_{3-\delta} + \text{Ce}_{0.8}\text{Sm}_{0.2}\text{O}_{2-\delta}$	Pechini method	Mixing	0.06 at 800	[119]
$\text{La}_{0.6}\text{Sr}_{0.4}\text{Co}_{0.2}\text{Fe}_{0.8}\text{O}_{3-\delta} + \text{Ce}_{0.8}\text{Sm}_{0.2}\text{O}_{1.9}$	Commercial (fuel cell materials)	Infiltration	0.12 at 750	[120]
50 wt. % $\text{La}_{0.6}\text{Sr}_{0.4}\text{Co}_{0.2}\text{Fe}_{0.8}\text{O}_{3-\delta} + \text{Ce}_{0.8}\text{Sm}_{0.2}\text{O}_{2-\delta}$	Microwave combustion	Mixing	2.77 at 800	[111]
50 wt. % $\text{La}_{0.6}\text{Sr}_{0.4}\text{Co}_{0.2}\text{Fe}_{0.8}\text{O}_{3-\delta} + \text{Ca}_{0.04}\text{Ce}_{0.96-x}\text{Sm}_x\text{O}_{2-\delta}$	Commercial (sigma aldrich)	Mixing	0.369 at 800	[121]
$\text{La}_{0.6}\text{Sr}_{0.4}\text{Co}_{0.2}\text{Fe}_{0.8}\text{O}_{3-\delta} + \text{La}_{0.8}\text{Sr}_{0.2}\text{MnO}_3$	Sol-gel (citrate complexing process)	Infiltration	2.1 at 700	[122]
$\text{La}_{0.8}\text{Sr}_{0.2}\text{Co}_{0.5}\text{Fe}_{0.5}\text{O}_3 + \text{YSZ}$	Impregnation solution	Infiltration	0.047 at 750	[123]
50 wt. % $\text{La}_{0.6}\text{Sr}_{0.4}\text{Co}_{0.2}\text{Fe}_{0.8}\text{O}_{3-\delta} + \text{BaCe}_{0.5}\text{Zr}_{0.35}\text{Y}_{0.15}\text{O}_{3-\delta}$	LSCF precursor solution-fiber	Electro spinning	0.299 at 700	[124]

Adding a pure ionic conducting material to pure electronic or MIEC cathode materials leads to electrical conductivity loss mainly due to the high ionic and low electronic conduction properties of the electrolyte materials. Our previous study showed that increasing the concentration of oxygen vacancies in the LSCF structure also increases the thermally-induced oxygen loss, which consequently decreases the oxygen concentration and electron carrier mobility [125]. In addition, LSCF-LSCF grain contact is substantially influenced by the electrical conductivity of the device, which markedly affects in-plane electronic conduction through the composite surface for the ORR and the overall ORR performance of the LSCF-based composite cathode. Furukawa et al. [126] claim that combining an LSCF cathode with a pure oxide ion conducting material lowers catalytic activity. The oxide ion conducting particles restrict the conduction path between LSCF-LSCF particle networks, increasing ohmic and charge transfer resistance. According to Fernandes et al. [127], a thin LSCF-based composite layer for current collection can improve LSCF-based composite cathode performance.

4. Concluding Remarks

For intermediate temperature SOFC (600–800 $^{\circ}\text{C}$), LSCF is a popular perovskite-structured MIEC cathode material due to its strong chemical stability, electrical property, and ORR catalytic activity. However, the major concerns for SOFC operations are the low surface electrocatalytic activity for the ORR at reduced operating temperature and microstructural instability of the LSCF cathode. Understanding how various factors affect the

microstructure of the cathode layer and consequently the LSCF cathode performance is necessary for improvement. This review illustrated how the composition and processing techniques affect the LSCF cathode microstructure and its performance. Each method exerts some influence on the electrical conductivity of the LSCF cathode depending on the powder properties and level of impurities. Therefore, optimal production method should be adopted to achieve maximum efficiency.

The performance of LSCF-based cathode materials can be remarkably enhanced through various strategies. This process involves the optimization of composition and microstructure by adopting suitable synthesis and fabrication conditions. Nano-structural design and surface modification through wet impregnation or infiltration can also substantially increase electrocatalytic operations, decrease ORR activation energy and ASR, and control the surface segregation and chemical reactivity of LSCF cathode. This process would dramatically encourage microstructural stability and tolerance under SOFC operating conditions to pollutants such as chromium, sulfur and boron. In addition, surface modification with LSM material and reduction of surface charge by doping with high-valence elements in the Sr and B-site can minimize or prevent Sr surface segregation and enhance the structural stability and electrochemical polarization. Understanding the interrelationships between the microstructure of the LSCF cathode layer and its performance is essential to realize optimal microstructures and maximize the ORR rate. These reviewed studies may represent a profound understanding of the synthesis, fabrication, and cation migration processes in the LSCF cathode. However, the rational architecture of the SOFC cathode can also be improved by sophisticated modeling and real-time interfacial simulations. The authors hope the details given in this review would be helpful and time-effective in accomplishing this ultimate objective.

Acknowledgement

This research was funded by Universiti Kebangsaan Malaysia (UKM) through the research grant: GGPM-2021-058.

References

- [1] Stambouli, A.B., Traversa, E. (2002). Solid oxide fuel cells (SOFCs): A review of an environmentally clean and efficient source of energy. *Renewable and Sustainable Energy Reviews*, 6, 5, 433-455.
- [2] Somalu, M. R., Muchtar, A., Daud, W. R. W., Brandon, N. P. (2017). Screen-printing inks for the fabrication of solid oxide fuel cell films: A review, *Renewable and Sustainable Energy Reviews*, 75, 426-439.
- [3] Dillig, M., Karl, J. (2012). Thermal management of high temperature solid oxide electrolyser cell/fuel cell systems. *Energy Procedia*, 28, 37-47.
- [4] Lund, P.D., Zhu, B., Li, Y., Yun, S., Nasibulin, A. G., Raza, R., Leskelä, M., Ni, M., Wu, Y., Chen, G., Fan, L., Kim, J.S., Basu, S., Kallio, T., Pamuk, I. (2017). Standardized Procedures Important for Improving Single-Component Ceramic Fuel Cell Technology. *ACS Energy Letters*, 2, 12, 2752-2755.
- [5] Panopoulos, K.D., Fryda, L.E., Karl, J., Poulou, S., Kakaras, E. (2006). High temperature solid oxide fuel cell integrated with novel allothermal biomass gasification. Part I: Modelling and feasibility study. *Journal of Power Sources*, 159, 570-585.
- [6] Hussain, A.M., Pan, K.-J., Robinson, I. A., Hays, T., Wachsman, E.D. (2016). Stannate-Based Ceramic Oxide as Anode Materials for Oxide-Ion Conducting Low-Temperature Solid Oxide Fuel Cells, *Journal of The Electrochemical Society*, 163, 10, F1198-F1205.
- [7] Abdalla, A M., Hossain, S., Azad, A.T., Petra, P.M.I., Begum, F., Eriksson, S.G., Azad, A.K. (2018). Nanomaterials for solid oxide fuel cells: A review. *Renewable and Sustainable Energy Reviews*, 82, 353-368.
- [8] de Larramendi, I. R., Ortiz-Vitoriano, N., Dzul-Bautista, I. B., Rojo, T. (2016). Designing Perovskite Oxides for Solid Oxide Fuel Cells, L. Pan, G. Zhu (Ed.), *Perovskite Materials - Synthesis, Characterisation, Properties, and Applications*, InTech, London, 589-617.
- [9] Aguadero, A., Fawcett, L., Taub, S., Woolley, R., Wu, K. T., Xu, N., Kilner, J. A., Skinner, S. J. (2012). Materials development for intermediate-temperature solid oxide electrochemical devices. *Journal of Materials Science*, 47, 9, 3925-3948.
- [10] Park, J., Kim, D., Baek, J., Yoon, Y.-J., Su, P.-C., Lee, S. (2018). Numerical Study on Electrochemical Performance of Low-Temperature Micro-Solid Oxide Fuel Cells with Submicron Platinum Electrodes. *Energies*, 11, 5, 1204.
- [11] Su, S., Gao, X., Zhang, Q., Kong, W., Chen, D. (2015). Anode- Versus Cathode-Supported Solid Oxide Fuel Cell : Effect of Cell Design on the Stack Performance. *International Journal of Electrochemical Science*, 10, 2487-2503
- [12] Fabbri, E., Licocchia, S., Traversa, E., Wachsman, E. D. (2009). Composite cathodes for proton conducting electrolytes. *Fuel Cells*, 9, 2, 128-138.
- [13] Li, Y., Gemmen, R., Liu, X. (2010). Oxygen reduction and transportation mechanisms in solid oxide fuel cell cathodes. *Journal of Power Sources*, 3345-3358.
- [14] Silva, C. L. S., Gama, L. M., Santos, J. A. F. dos, Paes Jr, H. R., Domingues, R. Z., Rangel, M. do C. (2017).

- Effect of La_{0.8}Sr_{0.2}MnO₃ powder addition in the precursor solution on the properties of cathode films deposited by spray pyrolysis. *Revista Matéria*, 22, 1, 1-10.
- [15] Kim, J.-H., Manthiram, A. (2015). Layered LnBaCo₂O_{5+δ} perovskite cathodes for solid oxide fuel cells: an overview and perspective. *J. Mater. Chem. A*, 3, 48, 24195-24210.
- [16] Liu, B., Zhang, Y. (2008). Status and prospects of intermediate temperature solid oxide fuel cells. *Journal of University of Science and Technology Beijing, Mineral, Metallurgy, Material*, 15, 1, 84-90.
- [17] Jeong, C., Lee, J. H., Park, M., Hong, J., Kim, H., Son, J. W., Lee, J. H., Kim, B. K., Yoon, K. J. (2015). Design and processing parameters of La₂NiO_{4+δ}-based cathode for anode-supported planar solid oxide fuel cells (SOFCs). *Journal of Power Sources*, 297, 370-378.
- [18] Pérez-Coll, D., Aguadero, A., Escudero, M. J., Daza, L. (2009). Electrochemical behavior of La₂Ni_{0.6}Cu_{0.4}O_{4+δ} oxide on SDC electrolyte as cathode for IT-SOFC. *ECS Transactions* (25), 2589-2596.
- [19] Lalanne, C., Mauvy, F., Siebert, E., Fontaine, M. L., Bassat, J. M., Ansart, F., Stevens, P., Grenier, J. C. (2007). Intermediate temperature SOFC single cell test using Nd_{1.95}NiO_{4+δ} as cathode. *Journal of the European Ceramic Society*, 27, 13-15, 4195-4198.
- [20] Wei, T., Huang, Y.-H., Zeng, R., Yuan, L.-X., Hu, X.-L., Zhang, W.-X., Jiang, L., Yang, J.-Y., Zhang, Z.-L. (2013). Evaluation of Ca₃Co₂O₆ as cathode material for high-performance solid-oxide fuel cell. *Scientific Reports*, 3, 1, 1125.
- [21] Kim, K. J., Park, B. H., Kim, S. J., Lee, Y., Bae, H., Choi, G. M. (2016). Micro solid oxide fuel cell fabricated on porous stainless steel: A new strategy for enhanced thermal cycling ability. *Scientific Reports*, 6, 1-8.
- [22] Yoo, S., Kim, J., Song, S. Y., Lee, D. W., Shin, J., Ok, K. M., Kim, G. (2014). Structural, electrical and electrochemical characteristics of La_{0.1}Sr_{0.9}Co_{1-x}Nb_xO_{3-δ} as a cathode material for intermediate temperature solid oxide fuel cells. *RSC Advance*, 4, 36, 18710-18717.
- [23] Xia, C., Liu, M. (2001). Low-temperature SOFCs based on Gd_{0.1}Ce_{0.9}O_{1.95} fabricated by dry pressing. *Solid State Ionics*, 144, 3-4, 249-255.
- [24] Huang, S., Peng, C., Zong, Z. (2008). A high-performance Gd_{0.8}Sr_{0.2}CoO₃-Ce_{0.9}Gd_{0.1}O_{1.95} composite cathode for intermediate temperature solid oxide fuel cell. *Journal of Power Sources*, 176, 1, 102-106.
- [25] Aguadero, A., Alonso, J. A., Pérez-Coll, D., de la Calle, C., Fernández-Díaz, M. T., Goodenough, J. B. (2010). SrCo_{0.95}Sb_{0.05}O_{3-δ} as Cathode Material for High Power Density Solid Oxide Fuel Cells. *Chemistry of Materials*, 22, 3, 789-798.
- [26] Li, M., Zhao, M., Li, F., Zhou, W., Peterson, V. K., Xu, X., Shao, Z., Gentle, I., Zhu, Z. (2017). A niobium and tantalum co-doped perovskite cathode for solid oxide fuel cells operating below 500 °C. *Nature Communications*, 8, 5, 1-9.
- [27] Zhou, W., Sunarso, J., Zhao, M., Liang, F., Klante, T., Feldhoff, A. (2013). A Highly Active Perovskite Electrode for the Oxygen Reduction Reaction Below 600 °C. *Angewandte Chemie International Edition*, 52, 52, 14036-14040.
- [28] Lee, S. J., Muralidharan, P., Jo, S. H., Kim, D. K. (2010). Composite cathode for IT-SOFC: Sr-doped lanthanum cuprate and Gd-doped ceria. *Electrochemistry Communications*, 12, 6, 808-811.
- [29] Zhao, F., Wang, X., Wang, Z., Peng, R., Xia, C. (2008). K₂NiF₄ type La_{2-x}Sr_xCo_{0.8}Ni_{0.2}O_{4+δ} as the cathodes for solid oxide fuel cells. *Solid State Ionics*, 179, 27-32, 1450-1453.
- [30] Kharlamova, T., Smirnova, A., Sadykov, V., Zarubina, V., Krieger, T., Batuev, L., Ishchenko, A., Salanov, A., Uvarov, N. (2008). Intermediate temperature solid oxide fuel cells based on nano-composite cathode structures. *ECS Transactions*, 13, 26, 275-284.
- [31] Pavlova, S., Kharlamova, T., Sadykov, V., Krieger, T., Muzykantov, V., Bepalko, Y., Ishchenko, A., Rogov, V., Belyaev, V., Okhlupin, Y., Uvarov, N., Smirnova, A. (2013). Structural Features and Transport Properties of La(Sr)Fe_{1-x}Ni_xO_{3-δ} - Ce_{0.9}Gd_{0.1}O_{2-δ} Nanocomposites—Advanced Materials for IT SOFC Cathodes. *Heat Transfer Engineering*, 34, 11-12, 904-916.
- [32] Shin, J. W., Go, D., Kye, S. H., Lee, S., An, J. (2019). Review on process-microstructure-performance relationship in ALD-engineered SOFCs. *Journal of Physics: Energy*, 1, 4, 042002.
- [33] Plonczak, P., Søgaard, M., Bieberle-Hütter, A., Hendriksen, P. V., Gauckler, L. J. (2012). Electrochemical Characterization of La_{0.58}Sr_{0.4}Co_{0.2}Fe_{0.8}O_{3-δ} Thin Film Electrodes Prepared by Pulsed Laser Deposition. *Journal of The Electrochemical Society*, 159, 5, B471.
- [34] Nityanand, C., Nalin, W. B., Rajkumar, B. S., Chandra, C. M. (2011). Synthesis and physicochemical characterization of nanocrystalline cobalt doped lanthanum strontium ferrite, *Solid State Sciences*, 13, 5, 1022-1030.
- [35] Hu, B., Wang, Y., Xia, C. (2015). Effects of Ceria Conductivity on the Oxygen Incorporation at the LSCF-SDC-Gas Three-Phase Boundary, *Journal of the Electrochemical Society*, 162, 1, F33-F39.
- [36] Almar, L., Szász, J., Weber, A., Ivers-Tiffée, E. (2017). Oxygen Transport Kinetics of Mixed Ionic-Electronic Conductors by Coupling Focused Ion Beam Tomography and Electrochemical Impedance Spectroscopy, *Journal of The Electrochemical Society*, 164, 4, F289-F297.
- [37] Sun, C., Hui, R., Roller, J. (2010). Cathode materials for solid oxide fuel cells: A review, *Journal of Solid State Electrochemistry*, 14, 7, 1125-1144.
- [38] Guo, S., Wu, H., Puleo, F., Liotta, L. (2015). B-Site Metal (Pd, Pt, Ag, Cu, Zn, Ni) Promoted

- La_{1-x}Sr_xCo_{1-y}FeyO_{3-δ} Perovskite Oxides as Cathodes for IT-SOFCs, *Catalysts*, 5, 1, 366-391.
- [39] Menzler, N. H., Tietz, F., Uhlenbruck, S., Buchkremer, H. P., Stöver, D. (2010). Materials and manufacturing technologies for solid oxide fuel cells, *Journal of Materials Science*, 45, 12, 3109-3135.
- [40] Richter, J., Holtappels, P., Graule, T., Nakamura, T., Gauckler, L. J. (2009). Materials design for perovskite SOFC cathodes, *Monatshefte für Chemie*, 140, 9, 985-999.
- [41] Burnwal, S. K., Bharadwaj, S., Kistaiyah, P. (2016). Review on MIEC Cathode Materials for Solid Oxide Fuel Cells, *Journal of Molecular and Engineering Materials*, 4, 2, 1-7.
- [42] Mahato, N., Banerjee, A., Gupta, A., Omar, S., Balani, K. (2015). Progress in material selection for solid oxide fuel cell technology: A review, *Progress in Materials Science*, 72, 141-337.
- [43] Maguire, E., Gharbage, B., Marques, F. M. B., Labrincha, J. A. (2000). Cathode materials for intermediate temperature SOFCs, *Solid State Ionics*, 127, 3, 329-335.
- [44] Skinner, S. J. (2001). Recent advances in Perovskite-type materials for solid oxide fuel cell cathodes, *International Journal of Inorganic Materials*, 3, 2, 113-121.
- [45] Zhu, L., Ran, R., Tadó, M., Wang, W., Shao, Z. (2016). Perovskite materials in energy storage and conversion, *Asia-Pacific Journal of Chemical Engineering*, 11, 3, 338-369.
- [46] Yang, Z., Guo, M., Wang, N., Ma, C., Wang, J., Han, M. (2017). A short review of cathode poisoning and corrosion in solid oxide fuel cell, *International Journal of Hydrogen Energy*, 42, 39, 24948-24959.
- [47] Jiang, S. P. (2019). Development of lanthanum strontium cobalt ferrite perovskite electrodes of solid oxide fuel cells – A review, *International Journal of Hydrogen Energy*, Elsevier Ltd, 7448-7493.
- [48] Athayde, D. D., Souza, D. F., Silva, A. M. A., Vasconcelos, D., Nunes, E. H. M., Da Costa, J. C. D., Vasconcelos, W. L. (2016). Review of perovskite ceramic synthesis and membrane preparation methods, *Ceramics International*, Elsevier, 6555-6571.
- [49] Huang, K., Zampieri, A., Ise, M. (2010). Cathode Polarizations of a Cathode-Supported Solid Oxide Fuel Cell, *Journal of The Electrochemical Society*, 157, 10, B1471.
- [50] Eciija, A., Vidal, K., Larrañaga, A., Martínez-Amesti, A., Ortega-San-Martín, L., Arriortua, M. I. (2013). Structure and properties of perovskites for SOFC cathodes as a function of the A-site cation size disorder, *Solid State Ionics*, 235, 14-21.
- [51] Adler, S. B. (2004). Factors Governing Oxygen Reduction in Solid Oxide Fuel Cell Cathodes †, *Chemical Reviews*, 104, 4791-4843
- [52] Bishop, S. R., Duncan, K. L., Wachsmann, E. D. (2009). Surface and Bulk Defect Equilibria in Strontium-Doped Lanthanum Cobalt Iron Oxide, *Journal of The Electrochemical Society*, 156, 10, B1242.
- [53] Hjalmarsson, P., Mogensen, M. (2011). La_{0.99}Co_{0.4}Ni_{0.6}O_{3-δ}-Ce_{0.8}Gd_{0.2}O_{1.95} as composite cathode for solid oxide fuel cells, *Journal of Power Sources*, 196, 17, 7237-7244.
- [54] Ullmann, H., Trofimenko, N., Tietz, F., Stöver, D., Ahmad-Khanlou, A. (2000). Correlation between thermal expansion and oxide ion transport in mixed conducting perovskite-type oxides for SOFC cathodes, *Solid State Ionics*, 138, 1-2, 79-90.
- [55] Wang, S., Katsuki, M., Dokiya, M., Hashimoto, T. (2003). High temperature properties of La_{0.6}Sr_{0.4}Co_{0.8}Fe_{0.2}O_{3-δ} phase structure and electrical conductivity, *Solid State Ionics*, 159, 1-2, 71-78.
- [56] Zhou, X., Anderson, H. U. (2004). Defect chemistry of p-type perovskite conductor used in solid oxide fuel cells, *Preprints of Papers- American Chemical Society, Division of Fuel Chemistry*, 49, 2, 749-750
- [57] Dutta, A., Mukhopadhyay, J., Basu, R. N. (2009). Combustion synthesis and characterization of LSCF-based materials as cathode of intermediate temperature solid oxide fuel cells, *Journal of the European Ceramic Society*, 29, 10, 2003-2011.
- [58] Tai, L. (1995). Structure and electrical properties of La_{1-x}Sr_xCo_{1-y}FeyO₃. Part 2. The system La_{1-x}Sr_xCo_{0.2}Fe_{0.8}O₃, *Solid State Ionics*, 76, 3-4, 273-283.
- [59] Tai, L. (1995). Structure and electrical properties of La_{1-x}Sr_xCo_{1-y}FeyO₃. Part 1. The system La_{0.8}Sr_{0.2}Co_{1-y}FeyO₃, *Solid State Ionics*, 76, 3-4, 259-271.
- [60] Habermeier, H. U. (2007). Thin films of perovskite-type complex oxides, *Materials Today*, 10, 10, 34-43.
- [61] Liu, Z., Han, M. F., Miao, W. T. (2007). Preparation and characterization of graded cathode La_{0.6}Sr_{0.4}Co_{0.2}Fe_{0.8}O_{3-δ}, *Journal of Power Sources*, 173, 837-841.
- [62] Petric, A., Huang, P., Tietz, F. (2000). Evaluation of La-Sr-Co-Fe-O perovskites for solid oxide fuel cells and gas separation membranes, *Solid State Ionics*, 135, 1-4, 719-725.
- [63] Tsvetkova, N. S., Zuev, A. Y., Tsvetkov, D. S. (2013). Investigation of GdBaCo_{2-x}FexO_{6-δ} (x = 0, 0.2) – Ce_{0.8}Sm_{0.2}O₂ composite cathodes for intermediate temperature solid oxide fuel cells, *Journal of Power Sources*, 243, 403-408.
- [64] Kim, Y.-M., Baek, S.-W., Bae, J., Yoo, Y.-S. (2011). Effect of calcination temperature on electrochemical properties of cathodes for solid oxide fuel cells, *Solid State Ionics*, 192, 1, 595-598.
- [65] Shao, Z., Zhou, W., Zhu, Z. (2012). Advanced synthesis of materials for intermediate-temperature solid oxide fuel cells, *Progress in Materials Science*, 57, 4, 804-874.
- [66] Hsu, C.-S., Hwang, B.-H. (2006). Microstructure and Properties of the La_{0.6}Sr_{0.4}Co_{0.2}Fe_{0.8}O₃ Cathodes Prepared by Electrostatic-Assisted Ultrasonic Spray Pyrolysis Method, *Journal of The Electrochemical Society*,

- 153, 8, A1478.
- [67] Ghouse, M., Al-Yousef, Y., Al-Musa, A., Al-Otaibi, M. F. (2010). Preparation of La_{0.6}Sr_{0.4}Co_{0.2}Fe_{0.8}O₃ nanoceramic cathode powders for solid oxide fuel cell (SOFC) application, *International Journal of Hydrogen Energy*, 35, 17, 9411-9419.
- [68] Leng, Y., Chan, S. H., Liu, Q. (2008). Development of LSCF-GDC composite cathodes for low-temperature solid oxide fuel cells with thin film GDC electrolyte, *International Journal of Hydrogen Energy*, 33, 14, 3808-3817.
- [69] Ge, L., Zhou, W., Ran, R., Shao, Z., Liu, S. (2008). Facile autocombustion synthesis of La_{0.6}Sr_{0.4}Co_{0.2}Fe_{0.8}O_{3-δ} (LSCF) perovskite via a modified complexing sol-gel process with NH₄NO₃ as combustion aid, *Journal of Alloys and Compounds*, 450, 1-2, 338-347.
- [70] Richardson, R. A., Cotton, J. W., Mark Ormerod, R. (2004). Influence of synthesis route on the properties of doped lanthanum cobaltite and its performance as an electrochemical reactor for the partial oxidation of natural gas., *Dalton transactions*, 3110-3115.
- [71] Tao, Y., Shao, J., Wang, J., Wang, W. G. (2008). Synthesis and properties of La_{0.6}Sr_{0.4}CoO_{3-δ} nanopowder, *Journal of Power Sources*, 185, 2, 609-614.
- [72] Babinić, S. M., Coker, E. N., Miller, J. E., Ambrosini, A. (2015). Investigation of La_xSr_{1-x}Co_yM_{1-y}O_{3-δ} (M (M = Mn, Fe) perovskite materials as thermochemical energy storage media, *Solar Energy*, 118, 451-459.
- [73] Świerczek, K. (2008). Thermoanalysis, nonstoichiometry and thermal expansion La_{0.4}Sr_{0.6}Co_{0.2}Fe_{0.8}O_{3-δ}, La_{0.2}Sr_{0.8}Co_{0.2}Fe_{0.8}O_{3-δ}, La_{0.9}Sr_{0.1}Co_{1/3}Fe_{1/3}Ni_{1/3}O_{3-δ} and La_{0.6}Sr_{0.4}Co_{0.2}Fe_{0.6}Ni_{0.2}O_{3-δ} perovskites, *Solid State Ionics*, 179, 1-6, 126-130.
- [74] Teraoka, Y., Nobunaga, T., Okamoto, K., Miura, N., Yamazoe, N. (1991). Influence of constituent metal cations in substituted LaCoO₃ on mixed conductivity and oxygen permeability, *Solid State Ionics*, 48, 3-4, 207-212.
- [75] Ushakov, S. V., Navrotsky, A., Weber, R. J. K., Neufeind, J. C. (2015). Structure and Thermal Expansion of YSZ and La₂Zr₂O₇ above 1500°C from Neutron Diffraction on Levitated Samples, *Journal of the American Ceramic Society*, 98, 10, 3381-3388.
- [76] Kharton, V. V., Kovalevsky, A. V., Viskup, A. P., Shaula, A. L., Figueiredo, F. M., Naumovich, E. N., Marques, F. M. B. (2003). Oxygen transport in Ce_{0.8}Gd_{0.2}O_{2-δ}-based composite membranes, *Solid State Ionics*, 160, 3-4, 247-258.
- [77] Qi, X., Lin, Y. S., Swartz, S. L. (2000). Electric transport and oxygen permeation properties of lanthanum cobaltite membranes synthesized by different methods, *Industrial and Engineering Chemistry Research*, 39, 3, 646-653.
- [78] Mostafavi, E., Babaei, A., Ataie, A. (2014). La_{0.6}Sr_{0.4}Co_{0.2}Fe_{0.8}O₃ perovskite cathode for intermediate temperature solid oxide fuel cells: A comparative study, *Iranian Journal of Hydrogen & Fuel Cell*, 4, 239-246.
- [79] Nie, L., Liu, Z., Liu, M., Yang, L., Zhang, Y., Liu, M. (2010). Enhanced Performance of La_{0.6}Sr_{0.4}Co_{0.2}Fe_{0.8}O_{3-δ} (LSCF) Cathodes with Graded Microstructure Fabricated by Tape Casting, *Journal of Electrochemical Science and Technology*, 1, 1, 50-56.
- [80] Shao, J., Tao, Y., Wang, J., Xu, C., Wang, W. G. (2009). Investigation of precursors in the preparation of nanostructured La_{0.6}Sr_{0.4}Co_{0.2}Fe_{0.8}O_{3-δ} via a modified combined complexing method, *Journal of Alloys and Compounds*, 484, 1-2, 263-267.
- [81] Zhou, W., Shao, Z., Ran, R., Gu, H., Jin, W., Xu, N. (2008). LSCF nanopowder from cellulose-glycine-nitrate process and its application in intermediate-temperature solid-oxide fuel cells, *Journal of the American Ceramic Society*, 91, 4, 1155-1162.
- [82] Garcia, L. M. P., Macedo, D. A., Souza, G. L., Motta, F. V., Paskocimas, C. A., Nascimento, R. M. (2013). Citrate-hydrothermal synthesis, structure and electrochemical performance of La_{0.6}Sr_{0.4}Co_{0.2}Fe_{0.8}O_{3-δ} cathodes for IT-SOFCs, *Ceramics International*, 39, 7, 8385-8392.
- [83] Mai, T. T. N., Ha, H. K. P., Thang, N. M. (2016). Synthesis La_{0.6}Sr_{0.4}Co_{0.2}Fe_{0.8}O_{3-δ} Perovskite by Microwave Assisted Sol – Gel Method and Properties of LSCF/GDC Composite Cathode for IT-SOFCs, *International Journal of Emerging Research in Management & Technology*, 5, 9, 13-19
- [84] Ge, L., Zhu, Z., Shao, Z., Wang, S., Liu, S. (2009). Effects of preparation methods on the oxygen nonstoichiometry, B-site cation valences and catalytic efficiency of perovskite La_{0.6}Sr_{0.4}Co_{0.2}Fe_{0.8}O_{3-δ}, *Ceramics International*, 35, 8, 3201-3206.
- [85] Ge, L., Ran, R., Shao, Z., Zhu, Z. H., Liu, S. (2009). Low-temperature synthesis of La_{0.6}Sr_{0.4}Co_{0.2}Fe_{0.8}O_{3-δ} perovskite powder via asymmetric sol-gel process and catalytic auto-combustion, *Ceramics International*, 35, 7, 2809-2815.
- [86] Liu, Y., Chen, K., Zhao, L., Chi, B., Pu, J. (2014). Performance stability and degradation mechanism of La_{0.6}Sr_{0.4}Co_{0.2}Fe_{0.8}O_{3-δ} cathodes under solid oxide fuel cells operation conditions, *International Journal of Hydrogen Energy*, 39, 28, 15868-15876.
- [87] Liu, M., Liu, Z., Liu, M., Nie, L. (2013). Fabrication and characterization of functionally-graded LSCF cathodes by tape casting, *International Journal of Hydrogen Energy*, 38, 2, 1082-1087.
- [88] Beckel, D., Muecke, U. P., Gyger, T., Florey, G., Infortuna, A., Gauckler, L. J. (2007). Electrochemical performance of LSCF based thin film cathodes prepared by spray pyrolysis, *Solid State Ionics*, 178, 5-6, 407-415.
- [89] Baqué, L., Serquis, A., Grunbaum, N., Prado, F., Caneiro, A. (2006). Preparation and Characterization of Solid Oxide Fuel Cells Cathode Films, *Mater. Res. Soc. Symp. Proc.*, 928, 1-6

- [90] Droushiotis, N., Torabi, A., Othman, M. H. D., Etsell, T. H., Kelsall, G. H. (2012). Effects of lanthanum strontium cobalt ferrite (LSCF) cathode properties on hollow fibre micro-tubular SOFC performances, *Journal of Applied Electrochemistry*, 42, 7, 517-526.
- [91] Harris, J., Kesler, O. (2009). Atmospheric Plasma Spraying Low-Temperature Cathode Materials for Solid Oxide Fuel Cells, *Journal of Thermal Spray Technology*, 19, 328-335.
- [92] Irshad, M., Siraj, K., Raza, R., Ali, A., Tiwari, P., Zhu, B., Rafique, A., Ali, A., Kaleem Ullah, M., Usman, A. (2016). A Brief Description of High Temperature Solid Oxide Fuel Cell's Operation, *Materials, Design, Fabrication Technologies and Performance*, Applied Sciences, 6, 3, 75.
- [93] Orera, V. M., Laguna-Bercero, M. A., Larrea, A. (2014). Fabrication Methods and Performance in Fuel Cell and Steam Electrolysis Operation Modes of Small Tubular Solid Oxide Fuel Cells: A Review, *Frontiers in Energy Research*, 2, 1-13.
- [94] Lee, S., Chu, C. L., Tsai, M. J., Lee, J. (2010). High temperature oxidation behavior of interconnect coated with LSCF and LSM for solid oxide fuel cell by screen printing, *Applied Surface Science*, 256, 6, 1817-1824.
- [95] Timurkutluk, B., Timurkutluk, C., Mat, M. D., Kaplan, Y. (2016). A review on cell/stack designs for high performance solid oxide fuel cells, *Renewable and Sustainable Energy Reviews*, 56, 1101-1121.
- [96] H. A. Taroco, J. A. F. Santos, R. Z. D. and T. M. (2011). Ceramic Materials for Solid Oxide Fuel Cells, *Advances in Ceramics - Synthesis and Characterization, Processing and Specific Applications* (45), InTech, 1548-1554.
- [97] Hedayat, N., Du, Y., Ilkhani, H. (2017). Review on fabrication techniques for porous electrodes of solid oxide fuel cells by sacrificial template methods, *Renewable and Sustainable Energy Reviews*, 77, , 1221-1239.
- [98] Gamble, S. (2011). Fabrication-microstructure-performance relationships of reversible solid oxide fuel cell electrodes-review, *Materials Science and Technology*, 27, 10, 1485-1497.
- [99] Baharuddin, N. A., Muchtar, A., Sulong, A. B., Abdullah, H. (2013). Fabrication methods for planar solid oxide fuel cells: A review, *Advanced Materials Research*, 662, July 2015, 396-401.
- [100] Zakaria, Z., Awang Mat, Z., Abu Hassan, S. H., Boon Kar, Y. (2020). A review of solid oxide fuel cell component fabrication methods toward lowering temperature, *International Journal of Energy Research*, 44, 2, 594-611.
- [101] da Conceição, L., Silva, A. M., Ribeiro, N. F. P., Souza, M. M. V. M. (2011). Combustion synthesis of La_{0.7}Sr_{0.3}Co_{0.5}Fe_{0.5}O₃ (LSCF) porous materials for application as cathode in IT-SOFC, *Materials Research Bulletin*, 46, 2, 308-314.
- [102] Möbius, A., Henriques, D., Markus, T. (2009). Sintering behaviour of La_{1-x}Sr_xCo_{0.2}Fe_{0.8}O_{3-δ} (0.3 ≤ x ≤ 0.8) mixed conducting materials, *Journal of the European Ceramic Society*, 29, 13, 2831-2839.
- [103] Kivi, I., Drovtar, I., Anderson, E., Aruväli, J., Tamm, K., Nurk, G., Möller, P., Vestli, M., Kanarbik, R., Lust, E. (2011). Influence of Cathode Thickness on the Oxygen Reduction Kinetics at the Intermediate Temperature SOFC Cathodes, *ECS Transactions* (7), 2349-2355.
- [104] Han, G. D., Neoh, K. C., Bae, K., Choi, H. J., Park, S. W., Son, J. W., Shim, J. H. (2016). Fabrication of lanthanum strontium cobalt ferrite (LSCF) cathodes for high performance solid oxide fuel cells using a low price commercial inkjet printer, *Journal of Power Sources*, 306, 503-509.
- [105] Liu, M., Liu, M., Ding, D., Blinn, K., Li, X., Nie, L. (2012). Enhanced performance of LSCF cathode through surface modification, *International Journal of Hydrogen Energy*, 37, 10, 8613-8620.
- [106] Laurencin, J., Hubert, M., Couturier, K., Le Bihan, T., Cloetens, P., Lefebvre-Joud, F., Siebert, E. (2015). Reactive Mechanisms of LSCF Single-Phase and LSCF-CGO Composite Electrodes Operated in Anodic and Cathodic Polarizations, *Electrochimica Acta*, 174, 1299-1316.
- [107] Shen, F., Lu, K. (2015). La_{0.6}Sr_{0.4}Co_{0.2}Fe_{0.8}O₃ cathodes incorporated with Sm_{0.2}Ce_{0.8}O₂ by three different methods for solid oxide fuel cells, *Journal of Power Sources*, 296, 318-326.
- [108] Shimura, K., Nishino, H., Kakinuma, K., Brito, M. E., Uchida, H. (2017). Effect of samaria-doped ceria (SDC) interlayer on the performance of La_{0.6}Sr_{0.4}Co_{0.2}Fe_{0.8}O_{3-δ}/SDC composite oxygen electrode for reversible solid oxide fuel cells, *Electrochimica Acta*, 225, 114-120.
- [109] Xu, Q., Huang, D. ping, Zhang, F., Chen, W., Chen, M., Liu, H. xing. (2008). Structure, electrical conducting and thermal expansion properties of La_{0.6}Sr_{0.4}Co_{0.8}Fe_{0.2}O_{3-δ}-Ce_{0.8}Sm_{0.2}O_{2-δ} composite cathodes, *Journal of Alloys and Compounds*, 454, 1-2, 460-465.
- [110] Shaula, A. L., Kharton, V. V., Marques, F. M. B., Kovalevsky, A. V., Viskup, A. P., Naumovich, E. N. (2006). Oxygen permeability of mixed-conducting composite membranes: Effects of phase interaction, *Journal of Solid State Electrochemistry*, 10, 1, 28-40.
- [111] Cesário, M. R., MacEdo, D. A., Martinelli, A. E., Nascimento, R. M., Barros, B. S., Melo, D. M. A. (2012). Synthesis, structure and electrochemical performance of cobaltite-based composite cathodes for IT-SOFC, *Crystal Research and Technology*, 47, 7, 723-730.
- [112] Muhammed Ali, S. A., Anwar, M., Raduwan, N. F., Muchtar, A., Somalu, M. R. (2018). Optical, mechanical and electrical properties of LSCF-SDC composite cathode prepared by sol-gel assisted rotary evaporation technique, *Journal of Sol-Gel Science and Technology*, 86, 2, 1-12.
- [113] Chen, J., Liang, F., Chi, B., Pu, J., Jiang, S. P., Jian, L. (2009). Palladium and ceria infiltrated La_{0.8}Sr_{0.2}Co_{0.5}Fe_{0.5}O_{3-δ} cathodes of solid oxide fuel cells, *Journal of Power Sources*, 194, 1, 275-280.

- [114] Zhao, E., Liu, X., Liu, L., Huo, H., Xiong, Y. (2014). Effect of $\text{La}_{0.8}\text{Sr}_{0.2}\text{Co}_{0.2}\text{Fe}_{0.8}\text{O}_{3-\delta}$ morphology on the performance of composite cathodes, *Progress in Natural Science: Materials International*, 24, 1, 24-30.
- [115] dos Santos-Gómez, L., Porras-Vázquez, J. M., Losilla, E. R., Martín, F., Ramos-Barrado, J. R., Marrero-López, D. (2017). Stability and performance of $\text{La}_{0.6}\text{Sr}_{0.4}\text{Co}_{0.2}\text{Fe}_{0.8}\text{O}_{3-\delta}$ nanostructured cathodes with $\text{Ce}_{0.8}\text{Gd}_{0.2}\text{O}_{1.9}$ surface coating, *Journal of Power Sources*, 347, 178-185.
- [116] dos Santos-Gómez, L., Porras-Vázquez, J. M., Losilla, E. R., Martín, F., Ramos-Barrado, J. R., Marrero-López, D. (2018). LSCF-CGO nanocomposite cathodes deposited in a single step by spray-pyrolysis, *Journal of the European Ceramic Society*, 38, 4, 1647-1653.
- [117] Gao, C., Liu, Y., Xi, K., Jiao, S., Tomov, R. I., Kumar, R. V. (2017). Improve the catalytic property of $\text{La}_{0.6}\text{Sr}_{0.4}\text{Co}_{0.2}\text{Fe}_{0.8}\text{O}_{3-\delta}/\text{Ce}_{0.9}\text{Gd}_{0.1}\text{O}_2$ (LSCF/CGO) cathodes with CuO nanoparticles infiltration, *Electrochimica Acta*, 246, 148-155. 8
- [118] Huang, T. J., Chou, C. L. (2010). Effect of voltage and temperature on NO removal with power generation in SOFC with V₂O₅-added LSCF-GDC cathode, *Chemical Engineering Journal*, 160, 1, 79-84.
- [119] Fu, C., Sun, K., Zhang, N., Chen, X., Zhou, D. (2007). Electrochemical characteristics of LSCF-SDC composite cathode for intermediate temperature SOFC, *Electrochimica Acta*, 52, 13, 4589-4594.
- [120] Nie, L., Liu, M., Zhang, Y., Liu, M. (2010). $\text{La}_{0.6}\text{Sr}_{0.4}\text{Co}_{0.2}\text{Fe}_{0.8}\text{O}_{3-\delta}$ cathodes infiltrated with samarium-doped cerium oxide for solid oxide fuel cells, *Journal of Power Sources*, 195, 15, 4704-4708.
- [121] Wang, B., Wang, Y., Fan, L., Cai, Y., Xia, C., Liu, Y., Raza, R., van Aken, P. A., Wang, H., Zhu, B. (2016). Preparation and characterization of Sm and Ca co-doped ceria- $\text{La}_{0.6}\text{Sr}_{0.4}\text{Co}_{0.2}\text{Fe}_{0.8}\text{O}_{3-\delta}$ semiconductor-ionic composites for electrolyte-layer-free fuel cells, *Journal of Materials Chemistry A*, 4, 40, 15426-15436.
- [122] Ai, N., Chen, K., Jiang, S. P. (2017). A $\text{La}_{0.8}\text{Sr}_{0.2}\text{MnO}_3/\text{La}_{0.6}\text{Sr}_{0.4}\text{Co}_{0.2}\text{Fe}_{0.8}\text{O}_{3-\delta}$ core-shell structured cathode by a rapid sintering process for solid oxide fuel cells, *International Journal of Hydrogen Energy*, 42, 10, 7246-7251.
- [123] Chen, J., Wan, D., Sun, X., Li, B. (2018). Interpretation of an inductive loop in the impedance of the impregnated $\text{La}_{0.6}\text{Sr}_{0.4}\text{Co}_{0.2}\text{Fe}_{0.8}\text{O}_{3-\delta}-\text{Y}_2\text{O}_3$ stabilized ZrO_2 cathodes, *Journal of Electroanalytical Chemistry*, 818, 1, 231-235.
- [124] Lee, S., Park, S., Wee, S., Baek, H. woo, Shin, D. (2018). One-dimensional structured $\text{La}_{0.6}\text{Sr}_{0.4}\text{Co}_{0.2}\text{Fe}_{0.8}\text{O}_{3-\delta}-\text{BaCe}_{0.5}\text{Zr}_{0.35}\text{Y}_{0.15}\text{O}_{3-\delta}$ composite cathode for protonic ceramic fuel cells, *Solid State Ionics*, 320, 347-352.
- [125] Muhammed Ali, S. A., Anwar, M., Ashikin, N., Muchtar, A., Somalu, M. R. (2018). Influence of oxygen ion enrichment on optical, mechanical, and electrical properties of LSCF perovskite nanocomposite, *Ceramics International*, 44, 9, 10433-10442.
- [126] Furukawa, N., Sameshima, S., Hirata, Y., Shimonosono, T. (2014). Influence of cathode on electric power of solid oxide fuel cells, *Journal of the Ceramic Society of Japan*, 122, 1423, 226-229.
- [127] Fernandes, A. de P. L., Garcia, E. M., de Almeida, R. M., Taroco, H. A., Silva, E. P. C., Domingues, R. Z., Matencio, T. (2016). Influence of cathode functional layer composition on electrochemical performance of solid oxide fuel cells, *Journal of Solid State Electrochemistry*, 20, 9, 2575-2580.